Development of Smart Tongue Devices for Measurement of Liquid Properties

Marina Cole, *Member, IEEE*, Gurmukh Sehra, Julian W. Gardner, *Senior Member, IEEE*, and Vijay K. Varadan

***Abstract*—In this paper, we describe the design and characterization of shear horizontal surface acoustic wave devices for the analysis of liquid samples. Devices were fabricated on both 36° rotated Y-cut X-propagating $LiTaO_3$ and $LiNbO_3$ substrates. The design consists of a dual delay-line configuration where one delay line is metallized and shielded, while the other is left electrically active. Experiments to characterize the devices in terms of sensitivity, temperature dependence, and mass loading have been conducted and the results presented. Different liquid samples, i.e., water, orange juice, and milk, are 100% linearly separable using principal components analysis. In addition, it is possible to measure the fat content ($\pm$0.1%) as well as the freshness of full (whole) milk.**

***Index Terms*—Shear horizontal surface acoustic wave (SH-SAW), smart tongue, 36YX.LT.**

I. Introduction

THE USE OF acoustic microsensors to detect the physical properties of liquids and gases, such as mass density and viscosity, offers the benefits of real-time electronic readout, small size, robustness, and low unit cost. By employing so-called chemical interfaces, the interaction of a chemical analyte with the sensor surface results in a change of propagating characteristics of the wave. While Rayleigh wave surface acoustic wave (SAW) sensors are the types of devices most commonly used in acoustic gas sensing applications, shear horizontal (SH) polarized waves are more suitable for liquid sensing [1]. For SH waves, the particle displacement is parallel to the surface and perpendicular to the wave propagation direction, so the losses associated with this type of device in liquids are not problematic. Here, we describe the design and characterization of a shear horizontal surface acoustic wave (SH-SAW) "smart tongue" devices fabricated on both 36° rotated Y-cut X-propagating $LiTaO_3$ (36YX.LT) and $LiNbO_3$ (36YX.LN) substrates employed for simultaneous measurements of both mechanical (acoustic) properties, and electrical (electroacoustic) parameters of the liquid under test. This is achieved through a dual delay-line configuration, one shorted (metallized and electrically shielded) and the other left free (electrically active). This way, apart from mass loading and viscosity (shorted delay line), it is possible to monitor additionally the permittivity and conductivity (free delay line) of the liquid under test parameters that can be related to taste properties, such as sweetness and saltiness. Furthermore, the approach adopted is based on a generic fingerprint correlated to key physical parameters, and so it does not employ a biochemical selective layer. This, in turn, increases the lifetime and durability of the resultant devices, albeit with a loss of specificity. This loss of specificity is not regarded as an issue for certain applications, e.g., rapid screening of milk freshness.

Manuscript received August 23, 2002; revised September 22, 2003. This work was supported by the Royal Society Research Grant 22277. The associate editor coordinating the review of this paper and approving it for publication was Dr. H. Troy Nagle.

M. Cole, G. Sehra, and J. W. Gardner are with the School of Engineering, University of Warwick, Coventry CV4 7AL, U.K. (e-mail: mvc@eng.warwick.ac.uk).

V. K. Varadan is with the Center for the Engineering of Electronic and Acoustic Materials and Devices, Pennsylvania State University, University Park, PA 16902 USA.

Digital Object Identifier 10.1109/JSEN.2004.832855

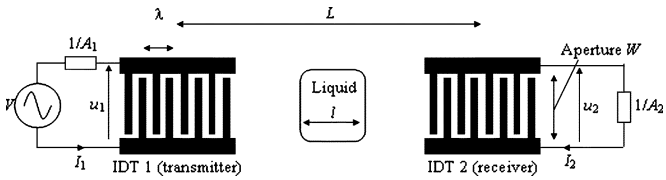

Fig. 1. Uniform interdigital transducer delay-line arrangement.

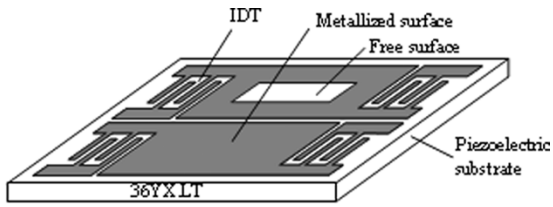

Fig. 2. Schematic drawing of a dual delay-line SH-SAW microsensor.

II. Operational Principle and Sensor Model

The basic principle of operation of the SH-SAW sensor in single free delay-line configuration is shown in Fig. 1. In this, input and output IDTs are connected to the source and the load with admittances A_1 and A_2, respectively. The first design principles and considerations are identical to those used for Rayleigh SAWs. The design of the IDTs for the generation and detection of SH-SAWs uses the delay-line configuration often employed for SAW filters [2]. Our sensor consists of two adjacent delay lines, with a thin layer of metal between the two IDTs on one delay line, representing an electrical short and the other delay line with a free nonmetallized surface area, as shown in Fig. 2. The basic operating principle utilized in the design of our liquid sensing devices is that perturbations that affect SH-SAW propagation on a metallized and electrically shorted surface are associated with the mechanical properties of the adjacent liquid, while SH-SAW propagating on a free surface are associated with both the mechanical and electrical

properties of the adjacent liquid [3]. The common environmental interactions elicit from both delay lines and can be removed by comparison between the two signals. The design is made considering analysis and prediction of the sensor response, which requires for the sensor effect to be accounted for in the device response. The sensor effect can be incorporated into the device unperturbed transfer function, to allow for the variations of delay time (related to phase shift) and attenuation.

Applying a voltage V across the two bus bars of the transmitter IDT, which are connected to identical finger pairs, a current I enters the electrodes. The current is determined by the static capacitance C of the electrodes and the acoustic admittance $G(\omega)+jB(\omega)$ of the IDTs caused by the generation of the SH-SAWs. The acoustic conductance $G(\omega)$ and acoustic susceptance $B(\omega)$ can be approximated as [3]–[5]

$$G(\omega) = G_0\left[\frac{\sin(\omega)}{\omega}\right]^2 \text{ and } B(\omega) = G_0\left[\frac{\sin(2\omega)-2\omega}{2\omega^2}\right]$$

where $\omega = \pi N((\omega-\omega_0)/\omega_0)$ and $G_0 = 2.25\omega_0 N^2 W(\varepsilon_0 + \varepsilon_p^T)(K^2/2)$. G_0 is the conductance at the center frequency ω_0, N is the number of fingers pairs, W is the aperture of the electrodes, ε_0 is the permittivity of vacuum, ε_p^T is the effective permittivity of the piezoelectric substrate, and K^2 is the electromechanical coupling coefficient of the substrate which depends on the crystal cut, frequency ω_0, and the mechanical properties and the thickness of the IDT metallization [4].

Then the input admittance $A_{11}(\omega)$ of the transmitter IDT is given by [4]

$$A_{11}(\omega) = \frac{I_1}{V} = G(\omega) + jB(\omega) + j\omega C. \tag{1}$$

Due to reciprocity, the input admittance of the receiver IDT, $A_{22}(\omega)$ is equal to $A_{11}(\omega)$.

Therefore, the complex unperturbed admittance transfer function for transmitter to receiver can be approximated as [4]

$$A_{12}(\omega) = \frac{I_2}{V} = G(\omega)\alpha\exp(-j\omega\tau_{\mathrm{SH}})$$

and $\tau_{\mathrm{SH}} = (L/v) = (L/(f\lambda))$ and $\omega = 2\pi f$, so

$$A_{12}(\omega) = G(\omega)\alpha\exp\left(-\frac{j2\pi L}{\lambda}\right) \tag{2}$$

where τ_{SH} is the delay time of the acoustic wave between the centers of the two transducers, α an attenuation coefficient for the acoustic waves, v is the phase velocity of the acoustic wave, λ is the wavelength, and L is the distance between the centers of the transducers.

The sensor effect, due to the presence of a liquid which causes a variation of the delay time and the attenuation of the SH wave, has to be included in this admittance transfer function as an additional phase shift and attenuation. Therefore, the perturbed admittance transfer function for the liquid sensor can be written as

$$A_{12}(\omega) = G(\omega)\alpha\exp\left(-\frac{j2\pi L}{\lambda}\right)\exp\left(\frac{j2\pi\delta l}{\lambda}\right)\exp(-al) \tag{3}$$

where $\delta = \Delta v/v$ is the fractional velocity change of the SH-SAW due to the sensing effect, l is the length of the liquid contact area, and a is the attenuation of the SH-SAW due to the sensor effect along the region of liquid contact l.

Thus, for the dual delay-line configuration of our sensors, we can represent the admittance transfer functions as

$$A_{s12}(\omega) = G_s(\omega)\alpha_s\exp\left(-\frac{j2\pi L}{\lambda}\right) \times\exp\left(\frac{j2\pi\delta_s l}{\lambda}\right)\exp(-a_s l) \tag{4}$$

$$A_{f12}(\omega) = G_f(\omega)\alpha_f\exp\left(-\frac{j2\pi L}{\lambda}\right) \times\exp\left(\frac{j2\pi\delta_f l}{\lambda}\right)\exp(-a_f l) \tag{5}$$

where the subscripts s and f represent the shorted delay line and free delay line, respectively. In terms of the voltage, the transfer function can be represented as

$$\frac{u_2}{V} = \frac{A_1 A_{12}}{A_{12}^2 - (A_1+A_{11})(A_2+A_{22})} \tag{6}$$

where A_1 and A_2 are external source and load admittances (see Fig. 1), respectively.

One parameter of interest of SAW devices is a measure of the attenuation given by the ratio of the output voltage and the reference voltage (voltage when source and load are directly connected). A measure of the attenuation is given by (u_2/u_{ref}) [4], where

$$\frac{u_{\mathrm{ref}}}{V} = \frac{A_1}{A_1+A_2}. \tag{7}$$

From (6) and (7), we get

$$\text{Attenuation } = \frac{u_2}{u_{\mathrm{ref}}} = \frac{A_{12}(A_1+A_2)}{A_{12}^2 - (A_1+A_{11})(A_2+A_{22})}. \tag{8}$$

The equations for the measurement of the power attenuation and phase shift can then be expressed as

$$\text{Attenuation A[dB]} = -20\log\left(\left|\frac{u_2}{u_{\mathrm{ref}}}\right|\right) \tag{9}$$

$$\text{Phase } \Delta\phi[\mathrm{deg}] = \arg\left(\frac{u_2}{u_{\mathrm{ref}}}\right). \tag{10}$$

A. Effects of External Environment

Acoustic wave devices are sensitive to a large number of physical and chemical measurands. These include such parameters as temperature, pressure, acceleration, stress, and the adjacent medium's density, viscoelastic properties, electrical permittivity, and electrical conductivity. Indeed, it is this range of measurand sensitivities that make acoustic wave devices attractive for a wide range of different sensing applications [6]. However, since one is usually interested in exploiting only one of these sensitivities for a particular application, all other responses become undesirable interferences. Thus, it is essential that the

sensor environment be carefully controlled to eliminate the effects of sensor cross sensitivities [1] and a difference and ratiometric principle adopted to remove common mode effects.

Temperature Effects: Temperature has a direct effect on the operation of all acoustic wave devices. A change in temperature produces a change in the density of the substrate (a direct effect of change in the length of the substrate), which, in turn, causes a change in velocity of the SH-SAW. For simplicity reasons, we are ignoring the temperature dependence of the Young's modulus. Since the change in wave velocity, along with the attenuation, is the parameter most commonly used in SAW sensors applications, there will be a temperature-dependent component associated with the sensor output signal. While efforts to identify substrates that have zero temperature coefficient have produced a significant reduction of temperature sensitivities, no substrate with negligible temperature coefficients that support SH-SAW are available in practice. Furthermore, physical properties of coating materials are often temperature dependent. Also, the liquid under test and the packaging material of the SAW sensor generally have different expansion coefficients than the device, which compounds the problem.

Assuming a linear thermal expansion in the substrate the acoustic path length L and the sensing length l will vary according to the linear relationship

$$L = L_0(1 + \kappa \Delta T) \tag{11}$$

where L_0 is the length at a reference temperature T_0, ΔT is the change in temperature $(T - T_0)$, κ is the expansion coefficient, and L is the length at actual temperature T.

A positive change in length ΔL will cause an increase in the delay time by $\Delta\tau$. Thus, the total delay time becomes $\tau_{\mathrm{SH}} + \Delta\tau$, where $\Delta\tau = ((\Delta L)/v) = ((\Delta L)/(f\lambda))$, and this can be approximated as

$$\tau_{\mathrm{SH}} + \Delta\tau \propto \frac{L + \Delta L}{f\lambda}.$$

Similarly, the sensing length l will also change due to the change in temperature to become $l + \Delta l$.

Substituting these changes in the expressions for the delay-line admittances [(4) and (5)], we get

$$\begin{aligned} A_{s_{12}}(\omega) = {} & G_s(\omega)\alpha_s \exp\left(-\frac{j2\pi(L+\Delta L)}{\lambda}\right) \\ & \times \exp\left(\frac{j2\pi\delta_s(l+\Delta l)}{\lambda}\right) \\ & \times \exp\left(-a_s(l+\Delta l)\right) \end{aligned} \tag{12}$$

$$\begin{aligned} A_{f_{12}}(\omega) = {} & G_f(\omega)\alpha_f \exp\left(-\frac{j2\pi(L+\Delta L)}{\lambda}\right) \\ & \times \exp\left(\frac{j2\pi\delta_f(l+\Delta l)}{\lambda}\right) \\ & \times \exp\left(-a_f(l+\Delta l)\right). \end{aligned} \tag{13}$$

From (12) and (13), it can be seen that both delay lines are affected by the changes in the temperature. The actual sensing effect or perturbation due to the liquid contact could be determined by taking the ratio of the sensing line (i.e., shorted delay line) to that of the reference (i.e., free delay line), eliminating the effect of temperature and other common external effects

$$\begin{aligned} \frac{A_{s_{12}}}{A_{f_{12}}} = \frac{G_s(\omega)\alpha_s}{G_f(\omega)\alpha_f} \exp\left(2\pi j(\delta_s - \delta_f)\left(\frac{l}{\lambda} + \frac{\Delta l}{\lambda}\right)\right) \\ \times \exp\left(-(a_s - a_f)(l + \Delta l)\right). \end{aligned} \tag{14}$$

Furthermore, by subtraction of the signals between the free and shorted lines, we can determine the signal that corresponds to the electrical properties from the free line which senses both the electrical and mechanical properties.

B. Liquid Perturbations

Acoustoelectric Interactions: The SH-SAW wave that propagates on the surface of $LiTaO_3/LiNbO_3$ substrates has an associated electric field that propagates several micrometers into a liquid. This electrical interaction (also known as the acoustoelectric interaction) with the liquid affects the velocity and/or attenuation of SH-SAW propagation, and it is utilized in sensing the dielectric properties of the liquids [2]. It has also been claimed that the high electromechanical coupling coefficients ($\sim$5%) of $LiTaO_3/LiNbO_3$ materials is a characteristic which enables SH-SAW sensors fabricated on these substrates to exhibit some specificity in detecting the electrical properties of an adjacent liquid [7].

When the surface is electrically shorted, the piezoelectric potential becomes zero, and, thus, only horizontally polarized shear displacement waves interact with the fluid. In this case, mechanical properties, including the viscosity and density, will be detected. On the other hand, the piezoelectric potential at the free surface extends to the liquid and subsequently measures additionally the complex dielectric properties, such as relative permittivity and conductivity [8].

By employing the perturbation theory proposed by Auld [9], the following acoustoelectric interaction (electrical) relationships for changes in velocity and attenuation of the SH-wave in the presence of a liquid are achieved

$$\frac{\Delta v}{v} = -\frac{K_s^2}{2}\frac{\left(\frac{\sigma'}{\omega}\right)^2 + \varepsilon_0\left(\varepsilon_r' - \varepsilon_r\right)\left(\varepsilon_r'\varepsilon_0 + \varepsilon_P^T\right)}{\left(\frac{\sigma'}{\omega}\right)^2 + \left(\varepsilon_r'\varepsilon_0 + \varepsilon_P^T\right)^2} \tag{15}$$

$$\frac{\Delta\alpha}{k} = \frac{K_s^2}{2}\frac{\left(\frac{\sigma'}{\omega}\right)\left(\varepsilon_r\varepsilon_0 + \varepsilon_P^T\right)}{\left(\frac{\sigma'}{\omega}\right)^2 + \left(\varepsilon_r'\varepsilon_0 + \varepsilon_P^T\right)^2}. \tag{16}$$

Here, K_s^2 is the electromechanical coupling coefficient when the reference liquid is loaded on the free surface, k is the wave number, ε_P^T is the effective permittivity of the SAW crystal, ε_r is the permittivity of the reference liquid (distilled water), and ε_r' and σ' are the permittivity and conductivity (related to loss)

of the measurand. From the above (15) and (16), we can determine circle formulae and by eliminating the conductivity and permittivity of the measurand from these formulae we can draw a permittivity-conductivity chart [8]

$$\left[\frac{\Delta v}{v}+\frac{K_s^2}{4}\frac{\varepsilon_0(2\varepsilon_r'-\varepsilon_r')+\varepsilon_P^T}{\varepsilon_r'\varepsilon_0+\varepsilon_P^T}\right]^2+\left[\frac{\Delta\alpha}{k}\right]^2 = \left[\frac{K_s^2}{4}\frac{\varepsilon_r\varepsilon_0+\varepsilon_P^T}{\varepsilon_r'\varepsilon_0+\varepsilon_P^T}\right]^2 \tag{17}$$

$$\left[\frac{\Delta v}{v}+\frac{K_s^2}{2}\right]^2+\left[\frac{\Delta\alpha}{k}-\frac{K_s^2}{4}\frac{\varepsilon_r\varepsilon_0+\varepsilon_P^T}{\frac{\sigma'}{\omega}}\right]^2 = \left[\frac{K_s^2}{4}\frac{\varepsilon_r\varepsilon_0+\varepsilon_P^T}{\frac{\sigma'}{\omega}}\right]^2. \tag{18}$$

Mechanical Interactions: SH-SAW propagating on a metal is perturbed by the mechanical properties of the adjacent liquid. The theory related to mechanical perturbation of SH-SAW on the metallized surface was developed by Kondoh *et al.* [3]. In this theory, the changes in the SH-SAW were derived from Auld's perturbation theory [9] for gases extending it to the liquid phase. The perturbation formula for a liquid sensor can be written as

$$\frac{\Delta\beta}{k}=-\frac{jv}{4\omega P}\left({v_p}^*\cdot Z' v_p+v_p\cdot Z^*\cdot {v_p}^*\right) \tag{19}$$

where k is the wave number, v is the phase velocity, ω is the angular frequency, P is the flow per unit width, v_p is the particle velocity vector, and Z is the acoustic metal surface impedance. Also, $'$ indicates a perturbed quantity and * indicates a complex conjugate. $\Delta\beta$ is the perturbation of the complex propagation constant β. β is defined in terms of k and the attenuation α as

$$\beta=k-j\alpha. \tag{20}$$

From (20), $\Delta\beta$ is given by

$$\frac{\Delta\beta}{k}=-\frac{\Delta v}{v}-j\frac{\Delta\alpha}{k}. \tag{21}$$

From (19) and (21), the change in the complex propagation constant can be decomposed into the changes of the velocity and the attenuation as

$$\frac{\Delta v}{v}=-\frac{v}{4\omega P}\left({v_p}^*\cdot Z_i'\cdot v_p-v_p\cdot Z_i\cdot {v_p}^*\right) \tag{22}$$

$$\frac{\Delta\alpha}{k}=-\frac{v}{4\omega P}\left({v_p}^*\cdot Z_r'\cdot v_p+v_p\cdot Z_r\cdot {v_p}^*\right) \tag{23}$$

where the subscripts r and i represent the real and imaginary parts of Z.

Viscous coupling: Assuming that a Newtonian fluid with a viscosity of η and density ρ_l is loaded on the metallized surface, by substituting the surface acoustic impedance Z into (22) and (23), we get

$$\frac{\Delta v}{v}=-\frac{v{v_{pc}}^2}{4\omega P}\left(\sqrt{\frac{\omega\eta'\rho_{l'}}{2}}-\sqrt{\frac{\omega\eta\rho_l}{2}}\right) \tag{24}$$

$$\frac{\Delta\alpha}{k}=\frac{v{v_{pc}}^2}{4\omega P}\left(\sqrt{\frac{\omega\eta'\rho_{l'}}{2}}+\sqrt{\frac{\omega\eta\rho_l}{2}}\right) \tag{25}$$

where v_{pc} is the particle velocity component of the shear horizontal mode.

Mass loading in liquid: Considering an isotropic thin film of thickness h and density ρ, uniformly loading the metallized surface in a liquid and that the liquid properties do not change before and after perturbation, the velocity shift and attenuation change can be obtained as

$$\frac{\Delta v}{v}=-\frac{uh{v_{pc}}^2}{4P}\left(\rho'-\frac{\mu'}{v^2}\right) \tag{26}$$

$$\frac{\Delta\alpha}{k}=0. \tag{27}$$

where μ' is the Lamè constant of the film. Equations (26) and (27) correspond to the Auld's equations for the gas phase [2], [9].

Thus, we can conclude that the changes in the velocity of SH-SAW on the two delays lines are functions of several parameters, some of them being common for both lines

$$\left(\frac{\Delta v}{v}\right)_{\text{free}}=f(\varepsilon,\sigma,\eta,\rho,T) \tag{30}$$

$$\left(\frac{\Delta v}{v}\right)_{\text{shorted}}=f(\eta,\rho,T) \tag{31}$$

where ε, σ, η, and ρ are the permittivity, conductivity, viscosity, and density of the liquid under test and T is the temperature common to both delay lines. It is these physical parameters that are being used to measure indirectly "taste" in our so-called electronic tongue.

III. Design and Fabrication

Several requirements have been taken into consideration in the design of the new SH-SAW liquid sensors. First, the size of the devices had to be determined. In order to measure easily the delay time difference between the two delay lines of the SH-SAW device, long delay lines and thus large devices are desirable. However, the sensitivity and rise time due to thermal properties are improved with smaller devices. Second, the number of transducer fingers for the new devices had to be determined. The bandwidth of the sensor output is mainly dependent on this number [10]. Increasing the number of fingers decreases the bandwidth. On the other hand, in order to minimize the device capacitance, the number of fingers should be kept low. However, to minimize conversion losses, the number of fingers should be high and diffraction losses can be kept to a minimum when the aperature is large [6], [11]. The maximum efficiency of coupling occurs when the width of the IDT fingers is equal to a quarter of the wavelength $w=\lambda/4$

TABLE I
DESIGN PARAMETERS OF SH-SAW SMART TONGUE DEVICES

Parameter	$LiTaO_3$	$LiNbO_3$
SH-SAW velocity *(v)*	4160 ms^{-1}	3488 ms^{-1}
Frequency of operation *(f)*	61.2 MHz	51.3 MHz
Wavelength of operation *(λ)*	68 μm	68 μm
Couping coefficient *(K^2)*	0.05	0.049
Spacing between fingers *(d)*	34 μm	34 μm
Width of IDT fingers *(w)*	17 μm	17 μm
IDT centre-centre separation *(L)*	7513 μm	7513 μm
IDT to IDT inside separation	5226 μm	5226 μm
Acoustic aperture *(W)*	2000 μm	2000 μm
Number of transducer fingers *(N)*	28	28
Time delay between IDTs *(t)*	1.26 μs	1.43 μs
Area of free surface ($l \times w$)	2×1.5 mm^2	2×1.5 mm^2
Overall size of device ($l \times w$)	10×7.5mm^2	10×7.5mm^2

and for the waves to be generated over a distance L (between the centers of the IDTs), the requirement for the acoustic aperture is $W \geq \sqrt{L\lambda}$. Thus, by choosing the aperture and the number of finger pairs, the transducer can be matched to a given input line, thus giving a low insertion loss for the device. The maximum relative bandwidth $((\Delta f)/f)$ over which the transducer can be matched is approximately proportional to $|K^2|$, the electromechanical coupling coefficient, and the optimum number of finger pairs N is proportional to $|(K^2)^{-1}|$ to allow the acoustic and electrical bandwidths to be made equal [10].

By considering all the above factors, the new SH-SAW devices were designed in a dual delay-line configuration and laid out on a 10 × 7.5 mm^2 die using the software package L-Edit (Tanner Tools). Parameters derived and used for the design of the smart tongue devices fabricated on both $LiTaO_3$ and $LiNbO_3$ substrates are summarized in Table I.

The devices were fabricated using a simple, well established process. First, both $LiTaO_3$ and $LiNbO_3$ wafers ($3''$) were cleaned in order to obtain good adhesion and uniform coating of metallic films. Next, the thin-metal films of chromium and gold with thickness of 20 and 120 nm, respectively, were deposited onto the wafers by thermal evaporation. Then, the four IDTs metallization and free area were photo-lithographically patterned with a $4''$ mask plate designed using the L-Edit (Tanner Tools) software package. Finally, chemical etching of the unwanted metal was performed, thus transferring the IDT designs onto the metallized wafers. The wafers were diced using a diamond dicing saw leaving the edges parallel to the IDT fingers fairly rough to minimize normal reflection of the backward travelling waves from the edge of the device back into the IDTs. The final device sizes were approximately 7.5 × 10 mm^2, as stated above. Fig. 3 shows a photograph of the fabricated device with an insert showing the individual IDT electrodes.

IV. EXPERIMENTAL METHOD

In order to test and characterize the SH-SAW sensors, the devices were mounted on a custom designed PCB and below a PTFE cell that contains the liquid under test. Fig. 4 shows a picture of the liquid cell. The cell is 32-mm long × 20-mm wide,

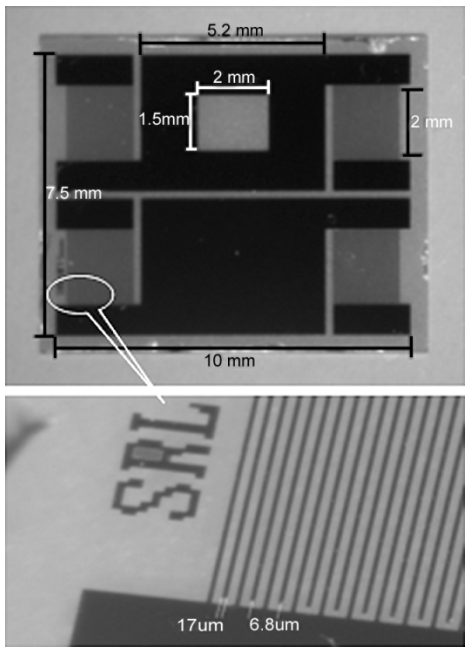

Fig. 3. Photograph of fabricated SH-SAW device.

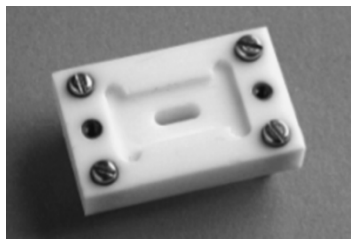

Fig. 4. Photograph of PTFE liquid cell.

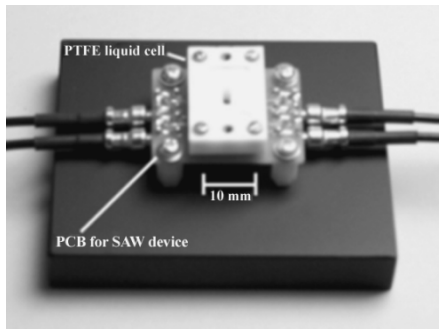

Fig. 5. Photograph of the assembled SH-SAW device with the PTFE liquid cell used for experimental setup.

with a central reservoir of 6.8 × 2.5 × 8 mm^3 and a volume of approximately 110 μl.

Fig. 5 shows a photograph of the test configuration. The liquid cell is positioned accurately over the sensing area between the IDTs with the aid of guiding pins that fit into holes in the PCB and rests on the device without any sealant. This enables easy removal of the cell to clean the device and yet hold the liquid samples without leaking.

The experimental procedure for SH-SAW devices involves the measurement of both the phase velocity and attenuation of the SH-SAW signals propagating on the delay lines of the

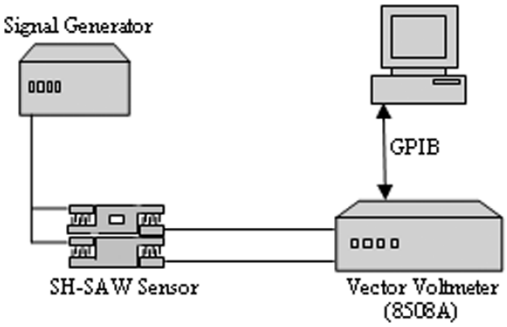

Fig. 6. Vector voltmeter measurement setup.

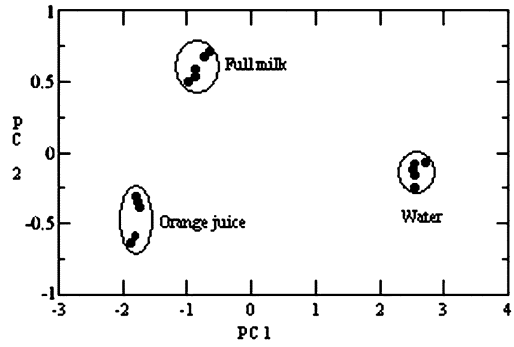

Fig. 7. Principal components analysis of different liquids showing excellent discrimination.

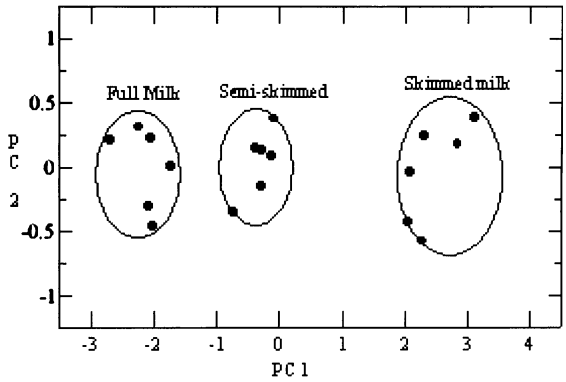

Fig. 8. Principal components analysis of different milks showing good discrimination.

sensor. The setup includes a signal generator, the SH-SAW sensor, and a vector voltmeter (HP 8505A). In this, an electrical signal is fed from the signal generator to the input IDTs; the amplitude ratio ΔA and phase difference $\Delta\phi$ between the input and output signals of each delay line were monitored by the vector voltmeter. The fractional velocity shift $\Delta v/v$ and attenuation change $\Delta\alpha/k$ of the SH-SAW can be derived from the phase difference and the amplitude ratio, respectively [6]. The basic experimental set up is shown in Fig. 6.

For the design parameters listed above, the frequency was found to be 61.18 MHz and, in practice, the center frequency was determined to be in the range of 61.0 to 61.2 MHz, suggesting an accurate fabrication process. Input impedance at the resonant frequency showed a close match with the external source and load of 50 Ω and the electrical bandwidth measured corresponded well with the calculated acoustic bandwidth of approximately 2 MHz. Also, the acoustic losses for the devices operating at this frequency, with a path length of approximately 5 mm, and a wavelength of around 68 μm, were found to be low, in the range of 6 to 15 dB for deionized (DI) water.

V. Results and Discussion

All the experiments conducted in order to test and characterize the SAW devices were performed under controlled temperature conditions of 23$\pm$0.1 °C using a commercial Dri-Bloc heater. Temperature characterization of the liquid sensors was performed and a linear dependence observed with temperature coefficients of $+0.1$ dB per degrees Celsius for attenuation loss and 0.9 degrees per degrees Celsius for phase shift observed for the $LiTaO_3$ free delay line.

After the initial characterization of the devices, experiments were conducted in order to discriminate between very different liquid samples (i.e., water, orange juice, and milk) and, hence, confirm our generic fingerprint approach in which the need for biochemical selective layers, normally used in liquid sensors, is removed. The experiments were performed by dispensing equal volumes (50 μl) of the different liquids into the microcell using a microliter syringe (cleaned and dried using DI water) to obtain five replicate measurements on each test liquid. The microcell and devices were cleaned and dried after each measurement using DI water. Results showing the discrimination of different liquid samples using the principal components analysis (PCA) technique, a linear, supervised, nonparametric pattern recognition method used to discriminate between the different samples under test [12], are presented in Fig. 7. The principle components are derived using four variables (sensor responses) measured using vector voltmeter setup, which are the attenuation A (in decibels) and phase difference $\Delta\phi$ (in degrees) on the shorted and free delay lines. Theoretical expressions for these parameters are given by (9) and (10) and from these equations, and (4) and (5), it can be seen that the measurements performed are directly related to the fractional change in phase velocity $\Delta v/v$ and attenuation change $\Delta\alpha/k$. These parameters can be related to the measured parameters by

$$\frac{\Delta v}{v} = -\frac{1}{360}\left(\frac{\lambda}{l}\right)\Delta\phi$$

$$\Delta\alpha = c_k\frac{\mathrm{A}}{l}$$

where l is the propagation path length in liquid and coefficient c_k is a function of the acoustic wavenumber k.

The fractional change in phase velocity $\Delta v/v$ and attenuation change $\Delta\alpha/k$ are the result of perturbations of the SH-SAWs propagating on a substrate surface caused by mechanical and/or electrical properties of the liquid under test and, therefore, are functions of these properties as derived in Section II and summarized by (30) and (31). Thus, the measured parameters A and $\Delta\phi$ can, in turn, be related to the viscosity, density, permittivity, and conductivity of the liquid under test, via conductivity-permittivity charts and using (17) and (18). This explains the physical principle underpinning our generic fingerprint approach.

Further tests on commercial milk samples with different fat content (whole milk with 4% fat, semi-skimmed with 2% fat,

TABLE II
FISHER t VALUES ON PREPROCESSED MILK DATA TO DETERMINE THE BEST SEPARATION COMBINATION

Pre-processing parameter				
Fisher t values	**AF-AS**	**PF-PS**	**AF / AS**	**PF / PS**
s - ss	3.16	4.31	-0.11	10.23
ss - ff	4.74	-1.19	-1.89	1.16
s - ff	6.25	1.53	-1.56	7.47

and skimmed milk with no fat) were performed followed by the dilution tests in which the dilution of whole milk using distilled de-ionized water was monitored. Fig. 8 shows the clear linear discrimination of milk samples with different fat content using principal components analysis.

An attempt to preprocess the data to improve the separation between the different milk samples is made by taking both the difference and ratio of the attenuations and phase differences on each of the delay lines, which also reduces the number of parameters involved to simply two. Then, a Fisher t test is performed on the sample means of two populations at a time (e.g., skimmed and semi-skimmed milk) for testing the equality of the two population means based on the independent samples from the two populations. The test statistic is given by

$$t = \frac{(\overline{x}_1 - \overline{x}_2)}{S_p \sqrt{\frac{1}{n_1} + \frac{1}{n_2}}} \tag{32}$$

where $\overline{x}_1$ and $\overline{x}_2$ are the sample means, n_1 and n_2 are the sample numbers, and S_p^2 is the pooled estimate of the population variance of the Fisher t test and is given by

$$S_p^2 = \frac{(n_1 - 1)S_1^2 + (n_2 - 1)S_2^2}{(n_1 + n_2 - 2)} \tag{33}$$

where S is the adjusted standard deviation.

The tests were performed on the different milk data and the results are displayed in Table II as Fisher t values for each of the variables (attenuation and phase on delay lines) for the preprocessed data, where s denotes skimmed milk, ss denotes semi-skimmed milk, and ff denotes full fat milk. The confidence level is found from standard statistical tables and for the eight degrees of freedom $(\mathrm{n_1} + \mathrm{n_2} - 1)$ here is better than 99.5% $(\mathrm{t} = 4.5)$ in several cases. Thus, having computed all the t values, the highest value of 10.23 indicates the best separation between the different samples and the associated preprocessing parameter was chosen to plot the data. This corresponds to a plot of the phase difference ratio $(\Delta\phi_\mathrm{F}/\Delta\phi_\mathrm{S})$ versus the attenuation difference $(\mathrm{A_F} - \mathrm{A_S})$ in decibels, shown in Fig. 9. The solid line represents a least-squares regression through the data points while the two dashed lines are orthogonal to the regression line and represent two hyperplanes that can be used to classify the milk samples with a simple parametric test.

As stated above, the best combination for separation is the difference ratio $(\Delta\phi_\mathrm{F}/\Delta\phi_\mathrm{S})$ versus attenuation difference $(\mathrm{A_F} - \mathrm{A_S})$ in decibels, where the attenuation difference in decibels is essentially the log of the ratio of the two signals. This agrees with the theory presented in Section II-A (14) which suggests that taking the ratio of the two signals removes the common external effects, hence giving the best separation as seen above.

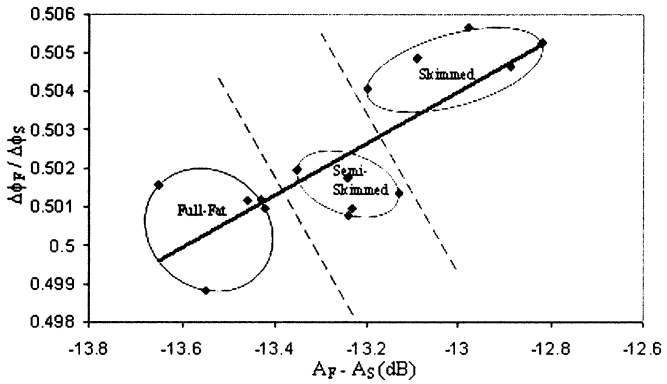

Fig. 9. Discrimination of different milks using the best combination of preprocessed data.

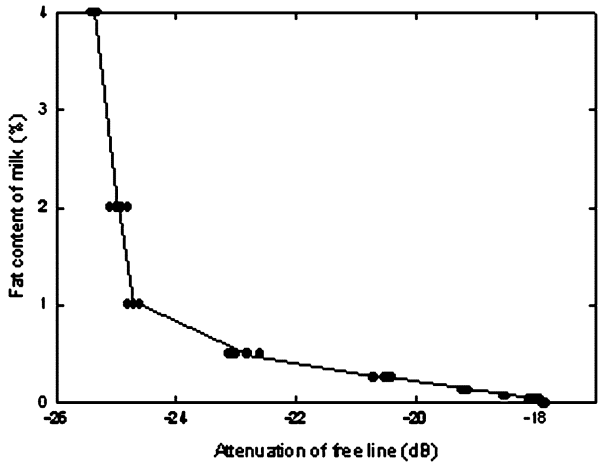

Fig. 10. Effect of milk fat content on attenuation loss of 36YX.LT free delay line.

In the dilution experiments, the concentration of the milk was diluted in stages by a factor of 2^n where n varied from 1 to 6. Each time, the volume of DI water was increased by a factor of 2^n and added to a fixed volume of whole milk. Equal volumes of the mixtures (60 μl) where dispensed into the liquid cell using a microliter syringe and the device and cell cleaned and dried after each sample was tested using DI water. The measurements were repeated randomly and five replicate measurements were conducted on each sample. Results are shown in Fig. 10 for the most sensitive parameter that is the attenuation of the free delay line, where the dilution step has been converted to the approximate percentage of fat in the milk where full cream milk is 4% and pure DI is 0%. From the graph, we estimate that the limit of detection of the free delay-line loss is *ca.* 0.1% of fat content.

Finally, tests investigating the freshness of whole milk samples were conducted. The fresh full milk was bought from the same supplier on five consecutive days and stored in a refrigerator at 23.8 °C in glass-covered containers (removed from original packaging). They were stored at a higher temperature than normal (refrigerated) in order to accelerate the growth of bacteria and, hence, the process of the milk going curdling. The measurements were then performed on the fifth day on all of the five samples. Again the samples were tested at random to obtain five replicate measurements of each sample for each day. The devices were washed out using DI water and dried after each

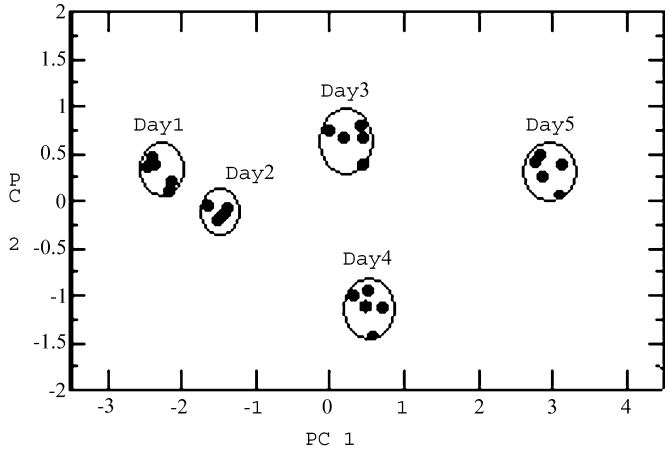

Fig. 11. Principal components analysis of milk samples showing the effect of aging.

measurement. Amount of 50 μl of milk samples was dispensed onto the devices each time. Fig. 11 shows five distinct clusters one for each day that the milk was tested.

VI. Conclusion

SH-SAW sensors have been fabricated and tested for use in a smart tongue. The ability to discriminate between three different liquids has been demonstrated confirming that the generic approach adopted removes the need for the use of biological selective layers. Tests to discriminate between milk samples with different fat content as well as a dilution test were also conducted and results were very encouraging with a sensitivity of about 0.1% fat content. Statistical analysis performed on the preprocessed data has confirmed that the dual delay-line configuration is a very effective concept in eliminating common mode effects. Also, extremely promising results were obtained on the milk freshness test, showing possible application of our liquid sensors as milk freshness indicators in dairy industry. Further tests will be conducted on device-to-device repeatability and possible applications in screening of clinical samples.

Acknowledgment

The authors would like to thank Z. Cui and G. Thomas of Rutherford Appleton Laboratory, Didcot, U.K., for the fabrication of the devices.

References

[1] D. S. Ballantine, R. M. White, S. J. Martin, A. J. Ricco, E. T. Zellers, G. C. Frye, and H. Wohltjen, *Acoustic Wave Sensors Theory, Design, and Physico-Chemical Applications*. New York: Academic, 1997.

[2] F. Josse, F. Bender, and R. W. Cernosek, "Guided shear horizontal surface acoustic wave sensors for chemical and biochemical detection in liquids," *Anal. Chem.*, vol. 73, pp. 5937–5944, 2001.

[3] J. Kondoh, K. Saito, S. Shiokawa, and H. Suzuki, "Simultaneous measurements of liquid properties using shear horizontal surface acoustic wave sensors," *Jpn. J. Appl. Phys.*, pt. 1, vol. 35, no. 5B, 1996.

[4] A. Leidl, I. Oberlack, U. Schaber, B. Mader, and S. Drost, "Surface acoustic wave devices and applications in liquid sensing," *Smart Mater. Struct.*, vol. 6, 1997.

[5] H. Drobe, A. Leidl, M. Rost, and I. Ruge, "Acoustic sensors based on surface-localized HPSWs for measurements in liquids," *Sens. Actuators A*, pp. 141–148, 1993.

[6] J. W. Gardner, V. K. Varadan, and O. O. Awadelkarim, *Microsensors MEMS and Smart Devices*. Chichester, U.K.: Wiley, 2001.

[7] J. Kondoh and S. Shiokawa, "New application of shear horizontal surface acoustic wave sensors to identifying fruit juices," *Jpn. J. Appl. Phys.*, pt. 1, vol. 33, no. 5B, pp. 3095–3099, 1994.

[8] V. K. Varadan and J. W. Gardner, "Smart tongue and nose," in *Proc. SPIE Conf. Smart Electronics and MEMS*, vol. 3673, Newport Beach, CA, 1999, pp. 67–75.

[9] B. A. Auld, *Acoustic Fields and Waves in Solids*, 2nd ed. Melbourne, FL: Krieger, 1990.

[10] A. J. Pointon, "Piezoelectric devices," *Proc. IEE* , vol. 129, pp. 298–307, 1982.

[11] M. Thompson and D. C. Stone, *Surface-Launched Acoustic Wave Sensors*. New York: Wiley, 1997.

[12] J. W. Gardner and P. N. Bartlett, *Electronic Noses Principles and Applications*. Oxford, U.K.: Oxford Univ. Press, 1999.

Marina Cole (M'98) received the B.Sc. degree from the University of Montenegro, Yugoslavia, and the Ph.D. degree from Coventry University, Coventry, U.K.

She joined the School of Engineering at Warwick University, Warwick, U.K., in 1996 as a Postdoctoral Research Assistant and she was appointed to a lectureship in electronic engineering in 1998. Her main research interests are integrated silicon-based sensors, SAW-based sensors, analog and mixed-signal ASICs, smart sensors, actuators, and microsystems.

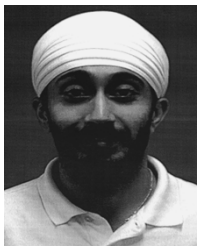

Gurmukh Sehra received the B.Eng. degree in electronic engineering from the University of Warwick, Warwick, U.K. in 2000. He is currently pursuing the Ph.D. degree at the Sensors Research Laboratory, University of Warwick.

He is a Postdoctoral Research Assistant at the Sensors Research Laboratory, University of Warwick. His main research interests are the design of surface acoustic wave devices for liquid and biosensing, remote sensing, the design of microantennas, and microfluidics.

Julian W. Gardner (M'91–SM'02) is Dean and Professor of electronic engineering at the School of Engineering, Warwick University, Warwick, U.K. He is author or coauthor of over 300 technical papers and patents, as well as six technical books in the area of microsensors and machine olfaction. He is a Series Editor for a book series by Wiley-VCH. He serves on several advisory panels on sensors, e.g., for EPSRC, DTI, and IEE Professional Network on Microsystems and Nanotechnology. He is on the Governing Body of Silsoe Research Institute, BBSRC. His research interests include the modeling of silicon microsensors, chemical sensor array devices, MEMS, and electronic noses. He has worked with over 20 companies in the past 15 years, developing commercial e-nose instruments and serving as a Consultant for various companies.

Prof. Gardner is a Fellow of the IEE. He is an Associate Editor of the IEEE Sensors Journal.

Vijay K. Varadan is an Alumni Distinguished Professor of engineering science, mechanics, and electrical engineering at the Pennsylvania State University, University Park. He is involved in all aspects of wave-material interaction, optoelectronics, microelectronics, photonics, and microelectromechanical systems (MEMS), including: nanoscience and technology, carbon nanotubes, and microstereolithography smart materials and structures; sonar, radar, microwave, and optically absorbing composite media; EMI, RFI, EMP, and EMF shielding materials; piezoelectric, chiral, ferrite, and polymer composites and conducting polymers; and UV conformal coatings, tunable ceramics materials and substrates, and electronically steerable antennas. He is the Editor of the *Journal of Wave-Material Interaction* and the Editor-in-Chief of the *Journal of Smart Materials and Structures* (Bristol, U.K.: IOP). He has authored more than 400 technical papers and six books. He holds eight patents pertinent to conducting polymers, smart structures and smart antennas, and phase shifters.